Scientific Reports

https://doi.org/10.1038/s41598-026-60590-y

Article in Press

Evaluating the copy capacity of polyvinylsiloxane molds in quantitative surface texture analysis of ground stone tools

Received: 19 November 2025

Accepted: 29 June 2026

Published online: 10 July 2026

Cite this article as: Sorrentino G., Paggi M., Longo L. *et al.* Evaluating the copy capacity of polyvinylsiloxane molds in quantitative surface texture analysis of ground stone tools. *Sci Rep* (2026). https://doi.org/10.1038/s41598-026-60590-y

Giusi Sorrentino, Marco Paggi, Laura Longo, Fabrizio Antonelli, Antonio Marcomini & Elena Badetti

Evaluating the Copy Capacity of Polyvinylsiloxane Molds in Quantitative Surface Texture Analysis of Ground Stone Tools

Giusi Sorrentino[1,2]; Marco Paggi[2*]; Laura Longo[1]; Fabrizio Antonelli[3]; Antonio Marcomini[1]; Elena Badetti[1]*

[1] DAIS, Department of Environmental Sciences, Informatics and Statistics, Ca' Foscari University of Venice, Via Torino 155, 30172 Mestre, Venice, Italy

[2] IMT School for Advanced Studies Lucca, Piazza San Francesco 19, 55100 Lucca, Italy.

[3] Iuav University of Venice, Dorsoduro 2206, 30125 Venice, Italy

** sorre.giusi@gmail.com; marco.paggi@imtlucca.it*

Abstract

Polyvinylsiloxane (PVS) is a molding compound originally developed for dental applications that, over the past 50 years, has also been widely used in archaeology to produce negative surface replicas of artifacts, owing to its excellent detail reproduction and dimensional stability. However, most studies assessing its replication accuracy have focused on bones, teeth, and flint tools, leaving ground stone tools (GSTs) largely unexplored. This study fills this gap by assessing the accuracy of PVS molding on GSTs, whose uneven surfaces and heterogeneous textures present particular challenges for both qualitative and quantitative analyses. We tested the accuracy and precision of PVS copies on a reference collection of GST replicas based on archaeological artifacts from Upper Paleolithic sites, representing four diverse lithologies. Confocal profilometry was used to acquire microtopographic maps of selected areas, enabling in-depth statistical comparisons between original surfaces and corresponding molds, with emphasis on key roughness descriptors. The results show that PVS molds effectively capture fine surface details, making them suitable for rough and irregular surfaces, though minor deviations and parameters overestimation must be considered in quantitative traceological analyses. By evaluating replication accuracy, this study contributes to the refinement of analytical methodologies for GSTs and improves the reliability of functional investigations.

Keywords: PVS mold, surface texture analysis, ground stone tools, confocal profilometer, statistical analysis.

INTRODUCTION

In archaeological research, the use of replicas for artifact analysis is a well-established practice. The study of surface textures and wear traces typically requires direct examination of the original objects; however, this is often limited by several constraints. These include restricted access to artifacts housed in museums, especially those located abroad, along with the logistical, legal, and financial challenges of transporting analytical equipment, when such instruments are even portable. Additionally, many microscopes are optimized for almost flat, lightweight and small samples, making the examination of large, heavy and irregular artifacts more difficult. For these reasons, the use of molds and casts to reproduce artifact surfaces has become an increasingly common practice. Molds facilitate transportation and analysis, as they are smaller, lighter, and not subject to the same restrictions as culturally significant artifacts. Over the past 50 years, polyvinylsiloxane (PVS) impression materials—originally developed for dental applications—have become widely adopted in archaeological and experimental contexts [e.g., 1-26]. This silicone-based compound is valued for its excellent fine-detail reproduction, as demonstrated on a wide variety of surfaces. Previous studies have reported its capability to capture microrelief features observable under magnifications up to 10,000× and with replication accuracy approaching the sub-5 µm scale [27-31]. In addition, PVS exhibits high tear strength, dimensional stability, and elastic recovery—properties that allow the molds to retain their original form and dimensions after deformation [32-33]. In anthropological and prehistoric artifact studies, several researchers have evaluated whether the accuracy of molding compounds in replicating surfaces is sufficient for texture analysis. Most of this research has focused on bones and teeth [1-2, 10, 34-40] and, to a lesser extent, on stone tools [12-13, 38, 41-43].

Also, in ground stone tool (GST) traceological analysis, high-definition PVS molds are widely used [e.g., 12-26]. Indeed, beyond overcoming the previously mentioned dimensional and transport constraints, molds can serve as a physical record of surface features that may be examined repeatedly and at later times, thus facilitating their sharing among researchers. This approach reduces direct handling of the original artifacts, thereby minimizing the risk of damage or contamination and enhancing accessibility for study. Moreover, during replicative experiments, molds enable the documentation of use-wear development, recording the successive stages of surface modification for subsequent examinations [24]. Molds allow a wide range of analyses, from low- to high-magnification imaging techniques [44] to profilometer measurements, and are also compatible with the vacuum conditions required for SEM [34]. The use of monochromatic molds enhances the examination of stone surface microtopography by improving contrast, allowing for a clearer analysis of morphological features. This approach overcomes potential misinterpretations caused by color variations in stones composed of multiple minerals. Furthermore, the translucency and reflectivity of stone crystals can complicate direct observation with optical instruments, whereas molds can mitigate these issues by providing a more uniform and opaque surface [14]. The reduced glare and improved color homogeneity enhance the visibility of surface textures and minimize light scattering during microscopic observation. Molds address structural constraints of analytical equipment, which are often not designed to accommodate large or irregularly shaped artifacts. For instance, the dimensions of GSTs frequently exceed the capacity of optical microscope stages or SEM chambers, and convex surfaces—such as those of pestles—are prone to movement during analysis. By providing stable, high-fidelity replicas, molds enable more precise and consistent microscopic and metrological analyses.

Despite these advantages, the accuracy of the impressions may be affected by the intrinsic texture of the molding compound, which has been reported to cause a general smoothing of the original surface [10, 12, 38]. Also, previous studies have emphasized that surface roughness significantly affects mold fidelity [38]. Furthermore, the molding process can trap air within the paste, creating circular smooth voids that, while easily identifiable across different scales and techniques, may still impact quantitative analyses. Although these issues are relevant, few studies have systematically evaluated the accuracy of molding compounds on uneven lithic surfaces, and only a limited number of feasibility assessments have been conducted to date [e.g., 12-13]. This limited research attention may be attributed to the unique challenges posed by GSTs for this type of application and analysis. Unlike flaked tools, which typically exhibit a uniform composition, smooth surfaces, and limited variation in raw materials and textures, GSTs display high variability across all these aspects. They are often composed of rocks with diverse mineral compositions and textural characteristics, resulting in significant differences in surface properties both within the same object and among artifacts. Moreover, GSTs frequently feature multiple working areas, each subjected to different degrees of use and functional tasks. This complexity requires careful planning of the molding strategy and a well-defined data acquisition design. Because different areas may record distinct use histories and exhibit varying levels of surface modification, the selection of the sampling zone is crucial. An inadequate or poorly structured strategy may result in loss of relevant information or introduce bias into the analysis, for example by producing data representative of only part of the artifact's functional history [25].

Building on this perspective, the present study aims to assess the accuracy and reproducibility of PVS molds in quantitative microtopography analysis. This evaluation was conducted across four different lithic types, encompassing a range of object geometries and surface textures. The samples consist of slabs and pebbles representing the primary lithologies documented at four Paleolithic sites, collected within the respective site catchment areas. Selection was based on compatibility in terms of lithology, shape, size, and weight, ensuring suitability as GST analogues in replicative plant-processing experiments. The sample set (Table 1) includes: a rectangular flat slab (DZU5_S) from Dzudzuana Cave, Caucasus, Georgia [45]; a large rectangular flat slab (OST1) from Ostuni 1, Italy [46]; an elongated ovoid pebble (BZ_M10) from Brînzeni I Cave, Moldova [47]; and a rounded, irregular pebble (Vi1) from Vindija Cave, Croatia [48]. This selection was carried out within the framework of broader research on the functional analysis of GSTs used by early modern humans during the Upper Paleolithic [22-25, 49]. Because these specimens represent lithologies and morphologies comparable to archaeological GSTs, they provided a suitable basis for assessing the performance of PVS molds in quantitative microtopography analysis under controlled conditions. Therefore, all samples were intentionally examined in their pristine, unused state as part of a methodological validation step. When tools are used to process biogenic materials, their surfaces may become coated with greasy films, and residues may penetrate surface porosity, affecting the interaction between the stone and the molding compound. Even after cleaning, third-body particles or residual films may persist and influence replication accuracy. Restricting the assessment to unused specimens allowed us to isolate the intrinsic performance of the molding material relative to the selected lithologies and to evaluate its performance for quantitative microtopographic measurements using confocal profilometry as the analytical technique.

Selected areas on the pebble surfaces were first scanned using a confocal profilometer, an optical technique that employs light to acquire microtopographic maps [25-50]. The same areas were then molded with PVS, and the corresponding regions on the molds were scanned under identical conditions and compared with those from the original stone surfaces. The analysis and comparison of the microtopographic maps were performed based on three spectral moments of the surface power spectral density (PSD): m_0, representing the variance of surface heights (first moment of the PSD); m_2, representing the variance of profile slopes (second moment); and m_4, representing the variance of asperity curvature (fourth moment) [51-53]. These statistical parameters are particularly relevant because they provide a quantitative description of surface roughness at multiple scales: m_0 reflects the overall amplitude of height variations, m_2 captures the sharpness and distribution of slopes, and m_4 characterizes the fine-scale curvature of surface asperities. From a traceological perspective, these moments allow for the assessment of surface modifications due to use, providing indications that help distinguish natural roughness from wear-induced alterations, thereby contributing to the interpretation of tool function.

RESULTS AND DISCUSSION

A preliminary petrographic characterization was performed to determine the lithology of the selected pebbles and slabs, as reported in Table 1.

Table 1. Morphometric and petrographic characteristics of the analyzed lithic samples.

Sample		Dimension (cm)	Thin section	Petrographic description	*Porosity (microscopic evaluation)
DZU5_S Dzudzuana Cave (Georgia, Caucasus)		12x8.8x2.8	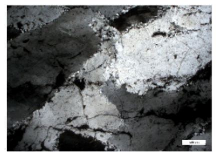	Intermediate-acid pyroclastic rock (dacite/rhyo-dacite) containing reddish scoriae, xenoliths of acid lavas and crystalline fragments (40-950 mm in size) of sericitised plagioclase, quartz, sanidine, pyroxene and opaque minerals (in descending order). The rock appears altered by hydrothermal fluids.	≥ 15%
OST1 Ostuni 1 site (Italy)		19.9x13.8x4.3	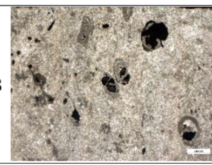	Marine limestone: bio-microsparite containing 10-15% vol. of bioclasts (micritised forminifera-miliolides and calcareous algae from 200 to 750 mm in size)	≈ 8% intraclastic
BZ_M10 Racovăț River, below Brînzeni I Cave (Moldova)		10x5.5x4.2	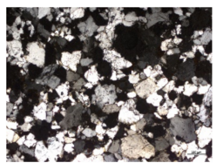	Very compacted quartz-arenite with scarce hematitic-argillaceous cement. It is composed of tightly packed quartz grains (≈ 95% vol., including chert and metamorphic quartz) with subordinate amounts of caolinized K-feldspar (pertite), plagioclase, rarer micas and oxides, traces of glauconite. Granule size: < 10 to 850 mm, with prevalence of the 30-40mm range.	≤ 5%
Vi1 Vindija Cave (Croatia)		8x5.3x3.2	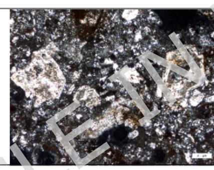	Medium to coarse-grained quartzite (prevailing crystalline grains around 2.5 mm in size) with traces of iron oxides and mica/sericite.	1-2%, intracrystalline

Initially, a qualitative evaluation was conducted to verify the molds' adherence to stone surfaces, their ability to penetrate pores and surface features, and the potential for bubble formation. A quartz-arenite pebble from Brînzeni I Cave, with the same petrographic characteristics as BZ_M10, was selected for this test. This stone presents an intermediate porosity (above 5%) among all the samples, making it a representative and suitable choice for evaluating PVS penetration into deep features across the four selected lithologies. The stone was molded and subsequently sawn without removing the mold. The resulting cross-section was examined under a stereomicroscope to observe the interface between the stone and the mold (Figure 1). The analysis revealed the presence of air bubbles, which in specific areas prevented the PVS from fully percolating into some surface valleys and pores. As a result, where a valley was present, the negative mold should have replicated it as a peak but instead reproduced it as a depression. Although this effect was limited to specific spots, overall adherence was found to be good from a qualitative imaging perspective, yielding promising results regarding the mold's replication capacity and encouraging further quantitative evaluation.

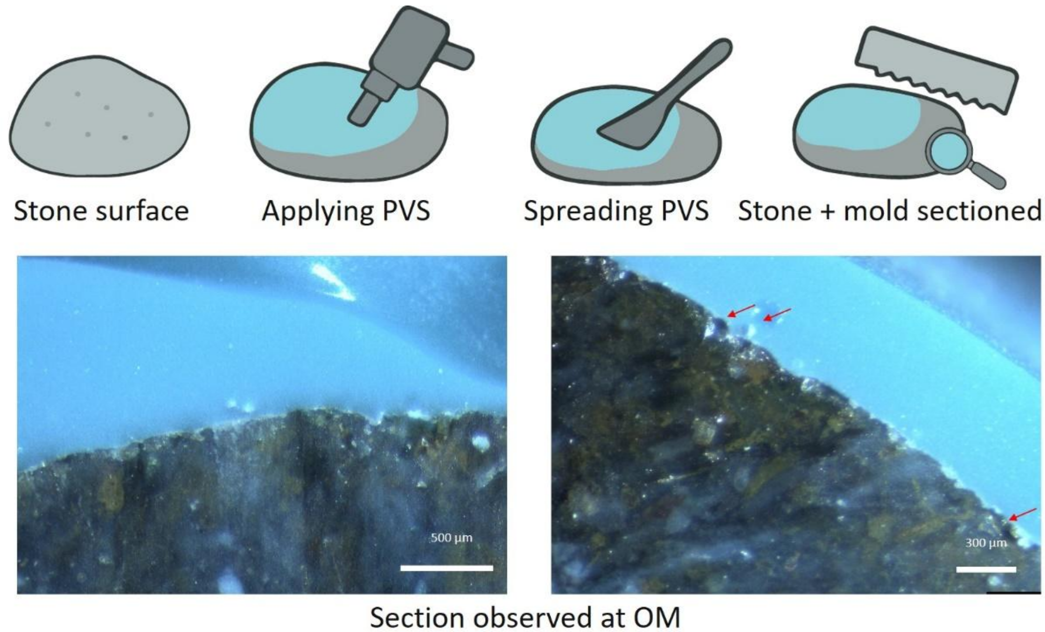

Figure 1. In the first row: schematic representation of the mold-making process: PVS is applied to the stone surface using an automixing gun, then spread evenly with a spatula. After curing, the stone with the applied mold was sawed, and the cross-section was examined under a stereomicroscope. In the second row: two micrographs showing the interface between the quartz-arenite pebble and the PVS mold, indicating a good overall adherence of the mold to the stone surface. Air bubbles (highlighted by red arrows) prevent complete penetration of the molding compound into surface valleys.

Building on this preliminary test, we extended the analysis to the four selected lithotypes (Table 1). On each pebble and slab, a specific region was selected and marked with an L-shaped engraving as a reference for microtopographic measurements. These regions were analyzed by confocal microscopy and profilometry through the acquisition of multiple areas along the reference mark, and were subsequently molded with PVS (see Supplementary Video for the molding procedure). After curing, the mold (designated as Mold 1) was peeled from the stone surface and also scanned. This procedure enabled direct quantitative comparison of approximately the same areas on the stone surfaces and their PVS replicas. Exact correspondence between the scanned areas could not be guaranteed, as relocation relied both on operator-controlled stage movement and visual judgment to identify the same areas on the stone and the mold. However, the L-shaped reference scratch ensured that the same predefined region was examined on both surfaces. The accuracy of the mold was assessed by calculating the three aforementioned statistical moments—m_0, m_2, and m_4—each reflecting a different aspect of surface topography. These parameters were calculated for both the individual scanned areas and the average values across all areas, thereby reducing the influence of minor spatial discrepancies on the overall results. The scatter plots below (Figures 2-4, 6-7) illustrate the relationship between the ten microtopographic areas measured on the original stone surfaces (x-axis) and the corresponding regions on the PVS molds (y-axis) for the four analyzed samples. Each plot displays the correlation between stone and mold values for a specific spectral moment. Black markers represent the ten measured areas for each specimen, while red ones indicate the mean value, with error bars showing one standard deviation (±σ) calculated from these ten measurements. This visualization enables a direct comparison of surface parameters between the original lithic artifacts and their mold replicas, highlighting the degree of correspondence and any systematic deviations.

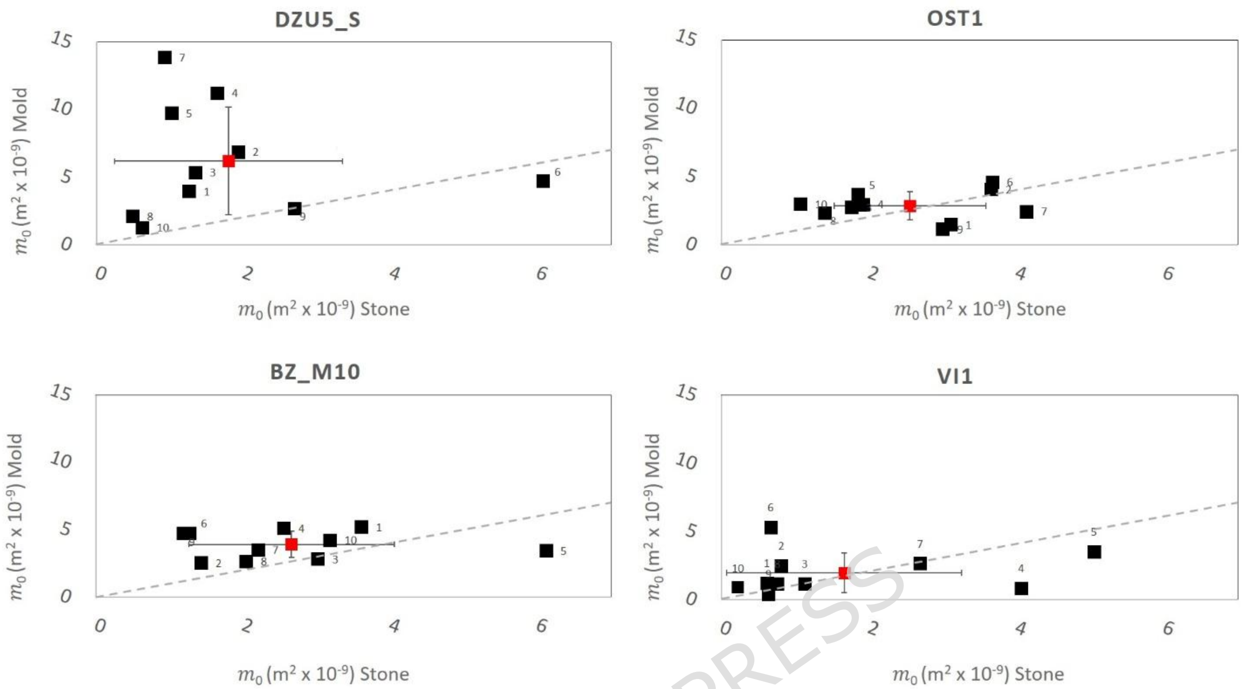

Figure 2. Scatter plots comparing the surface height variance (m_0) of the original lithic surfaces (x-axis) and their approximately corresponding regions on the PVS molds (y-axis) for the four analyzed samples. Black squares represent the ten measured microtopographic areas; red squares indicate the mean m_0 values, with error bars showing one standard deviation (±σ) calculated from these ten measurements. The dashed grey line corresponds to the 1:1 relationship between stone and mold values.

ARTICLE IN PRESS

The scatter plots in Figure 2 illustrate the results for the m_0 parameter, which represents the variance of surface heights. Although individual areas deviate to varying degrees from the 1:1 reference line, the mean values for most samples cluster around it, indicating overall agreement in the reproduction of vertical roughness between the molds and the original surfaces when considered as an ensemble. A slight overall tendency for the molds measurements to exceed those of the stones was observed, suggesting an overestimation of surface roughness in the measurements made on the PVS replicas.

These deviations are particularly evident for DZU5_S, where several measurements lie well above the 1:1 line, including some of the highest mold values among all samples. The mean value is clearly above the line of equality, and the error bars are among the largest. This likely reflects local imperfections in the molding process, such as air bubbles or incomplete filling of deeper valleys. However, this discrepancy may be attributable not only to the PVS replicas themselves, but also to the nature of the analytical technique—confocal profilometer—which is based on light reflection. In porous materials, as in this case, light may fail to fully penetrate narrow or deep cavities or return clear signals from their interiors, potentially leading to an underestimation of valley and pore depth. The PVS, by contrast, can percolate into these cavities, filling them. Upon curing, it forms a negative surface replica in which the filled depression becomes elevated features that are more easily captured by the confocal profilometer, contributing to the apparent amplification of roughness in the mold compared with the original stone scans. This effect is particularly evident for DZU5_S, as it is the most porous specimen. By contrast, OST1 displays the highest coherent correspondence, with most areas clustering tightly along the 1:1 line and the mean lying almost perfectly on it, indicating consistent reproduction of surface roughness. BZ_M10 also shows a good agreement, with both individual measurements and the mean only slightly above the line of equality, suggesting an overall accurate replication of topographic amplitude. Vi1 exhibits an intermediate behavior, with a broader dispersion and a few values slightly above the 1:1 line, likely reflecting localized enhancement of roughness on mold or the occasional presence of bubbles introduced during the molding process.

Overall, the results indicate that, despite local variability, the molding process effectively preserves the large-scale roughness characteristics of these lithic surfaces. However, reproducing the roughness of both the most porous and the least porous stones appears more challenging, as these materials show greater deviations from the line of equality.

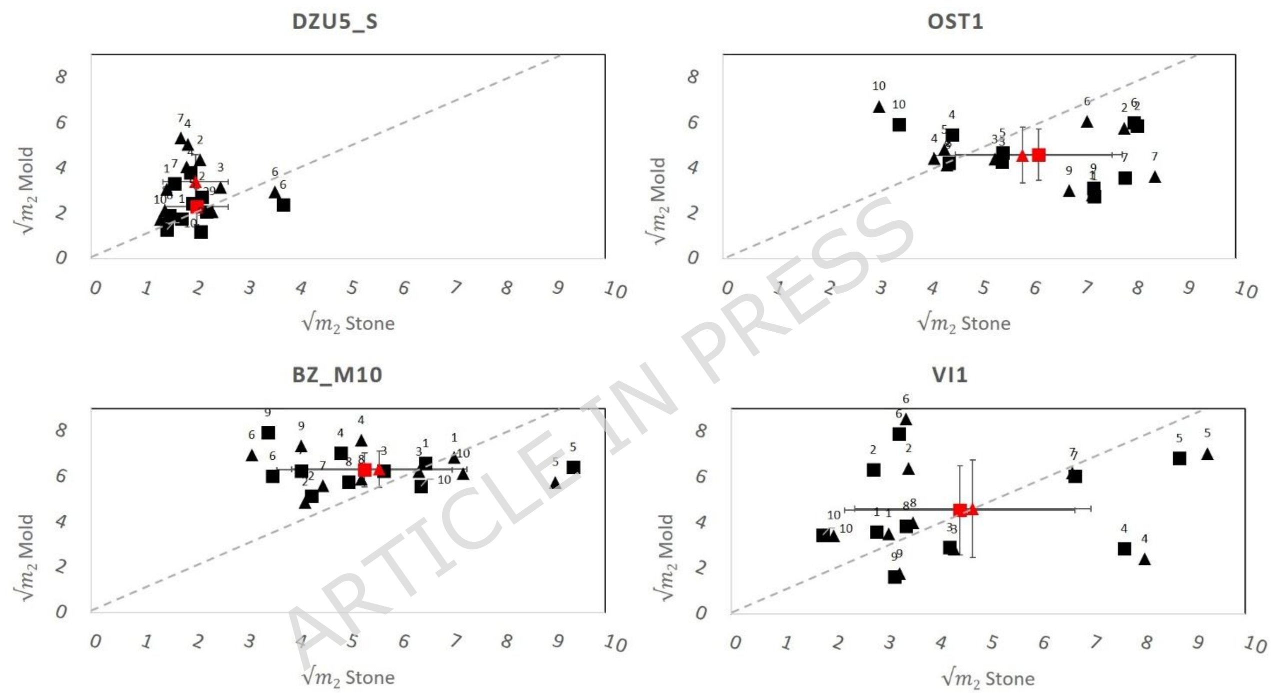

Figure 3. Scatter plots comparing the slopes variance (m_2) of the original lithic surfaces (x-axis) and their approximately corresponding regions on the PVS molds (y-axis) for the four analyzed samples. Black triangles and squares represent profiles extracted from the ten measured microtopographic areas along the x- and y-directions, respectively. Red markers indicate the mean m_2 values, with error bars representing one standard deviation (±σ) calculated from these ten measurements. The dashed grey line corresponds to the 1:1 relationship between stone and mold values.

The scatter plots in Figure 3 illustrate the results for the m_2 parameter, representing the variance of surface slopes computed along profiles extracted in both the x- (triangle markers) and y-directions (square markers). The original stones display very limited variation between the x and y directional slopes, indicating that their natural surfaces exhibit a high degree of isotropy—a characteristic generally well preserved in the PVS replicas. This provides an important baseline for functional analyses, as directional modifications could otherwise result from either tool use or post-depositional processes.

Overall, the molds replicate the original slope distribution with a high degree of statistical agreement at the ensemble level, rather than through exact spatial matching of individual scanned areas. DZU5_S, shows the lowest m_2 values among all specimens, reflecting limited slope variability. Mold values are slightly higher than those of the stone, suggesting a minor overestimation of slope variance but an excellent consistency among the ten analyzed areas. OST1 exhibits a wider dispersion, with some local over- and under-estimations, yet the mean lies close to the 1:1 line, indicating an overall accurate reproduction of surface gradients with moderate variability. BZ_M10 presents the best correspondence between stone and mold, as both individual data and mean values align very closely with the 1:1 relationship, reflecting a highly faithful replication of slope variance. Conversely, Vi1 shows greater scatter and larger standard deviations, indicating localized discrepancies in replication despite an average value close to the line of equality. These deviations may result from minor PVS deformation, small-scale heterogeneities in surface roughness, or slight misalignments between corresponding areas during profilometric scanning.

Overall, the results demonstrate that the PVS molds effectively reproduce the variance of surface slopes of these lithic surfaces, with only minor deviations attributable to small-scale molding imperfections or measurement uncertainties.

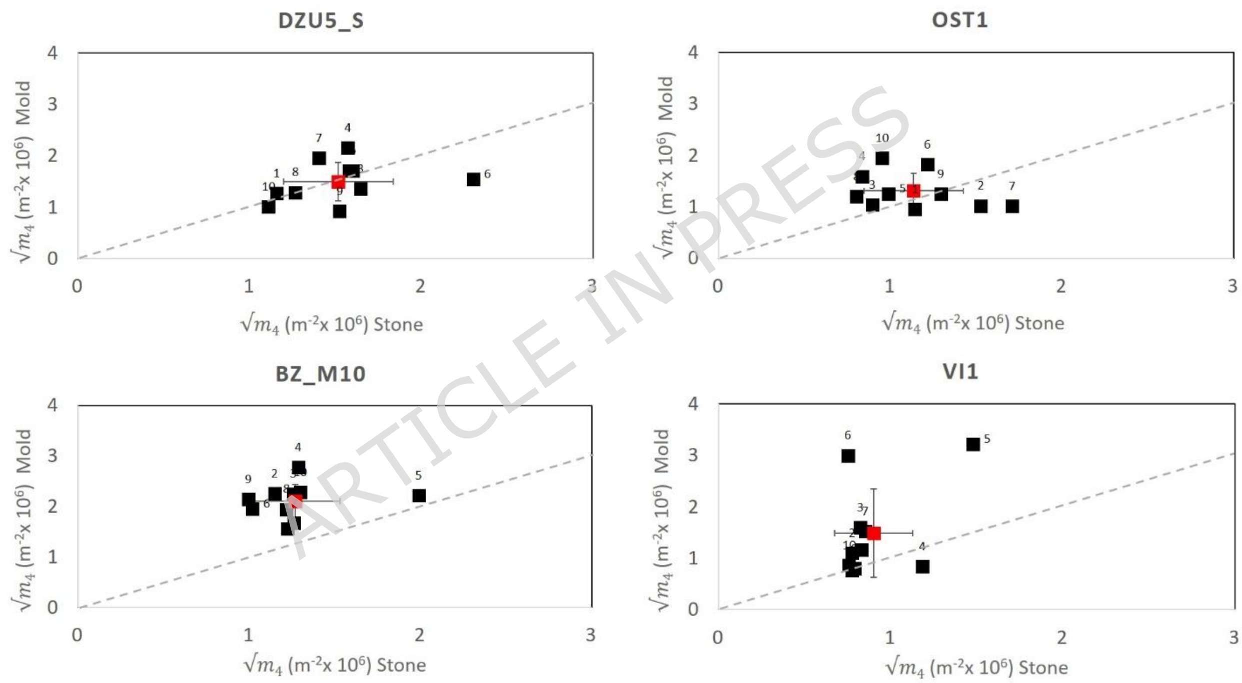

Figure 4. Scatter plots comparing the curvatures of the profile peaks variance (m_4) of the original lithic surfaces (x-axis) with their approximately corresponding regions on the PVS molds (y-axis) for the four analyzed samples. Black squares represent the ten measured microtopographic areas; red squares indicate the mean m_4 values, with error bars showing one standard deviation (±σ) calculated from these ten measurements. The dashed grey line corresponds to the 1:1 relationship between stone and mold values.

The scatter plots in Figure 4 illustrate the results for the m_4 parameter, representing the variance of profile-peak curvatures measured along profiles in the x direction. Overall, the PVS molds reproduce the curvature variance of the original lithic surfaces, though with slightly greater variability than that observed for the slope parameter (m_2).

Among the analyzed samples, DZU5_S shows the best correspondence between stone and mold, with most data points clustered close to the 1:1 line, values only slightly higher, and very limited dispersion. This indicates accurate replication of curvature characteristics, with only a minor systematic

overestimation of peak sharpness. OST1 exhibits a wider scatter, with both over- and underestimations, yet the mean remains close to the line of equality, reflecting a generally accurate reproduction of curvature features despite minimal variability. In contrast, BZ_M10 displays consistently higher mold values than those of the original stone, pointing to a systematic but modest overestimation of curvature variance. The narrow error bars, however, suggest that this bias is uniform and reproducible across the analyzed areas. Vi1, on the other hand, presents the largest dispersion and the highest standard deviations, with several mold measurements exceeding their correspondent stone's areas. This may reflect localized amplification of high-curvature features or, alternatively, misalignments between corresponding regions during profilometric scanning. As also observed for m_2, these discrepancies likely stem not only from the molding process but also from the optical nature of confocal profilometry. The instrument may underestimate sharp curvatures or deep valleys on the highly reflective quartz-based lithologies, while the PVS molds—having more diffuse reflectivity—allow for more complete surface capture.
The overall results indicate that the PVS molds reproduce peak variances with generally high fidelity, though fine-scale curvature features tend to show slightly greater amplification and variability than the broader slope characteristics captured by m_2.

Summarizing, across all statistical moments, the PVS molds demonstrate a high overall fidelity in replicating the microtopography of the four selected lithic surfaces. The variance of surface height is reproduced with good accuracy, though with a slight general tendency toward overestimating roughness, a behavior particularly evident in the most porous sample, DZU5_S. For the variance of slopes and curvatures, the correspondence between stone and mold remains generally high, indicating that both medium- and fine-scale surface features are effectively captured. However, small-scale curvature features (m_4) appear slightly more prone to amplification or variability than the broader-scale slope characteristics described by m_2, a tendency most marked in the highly reflective quartz-based sample Vi1. Overall, the molding process most faithfully reproduces the surfaces of the intermediate-porosity stones BZ_M10 and OST1, whereas deviations in Vi1 likely result more from optical interferences during profilometric scanning than from inaccuracies in the PVS replication itself.

In addition to the three statistical moments m_0, m_2, and m_4, the correspondence between the stone surfaces and their molds was further assessed through complementary analytical tools. Three-dimensional surface maps were generated to visualize the microtopographic variation across the measured areas, enabling direct visual–spatial comparison between the original stones and their PVS replicas. The relationship between surface asperities (3D maxima) heights and their curvatures was explored using contour plots of the related joint probability density function [53-54]. Furthermore, histograms were used to describe the probability density functions of the asperity heights and their curvatures. Figure 5 presents an example of these surface analyses for sample BZ_M10, area 10, showing both the stone and its corresponding mold area. The comparison demonstrates that the PVS replica faithfully reproduces both the large-scale morphology and the fine-scale roughness of the original surface. The height distributions (Figure 5 A, E) and 3D maps (Figure 5 C, G) exhibit nearly identical patterns, with only slight increases in the height range on the mold, indicating a minor amplification of relief. The few spikes visible near the edges of the reconstructed microtopography in Figure 5G, and, to a lesser extent, those in Figure 5C, correspond to boundary outliers that were not smoothed by the filter implemented in the analysis algorithm (see the *Data Processing and Statistical Analysis* paragraph in the *Materials and Methods* section). The curvature–height joint probability density contour plots (Figure 5 B, F) and curvature probability distributions (Figure 5 D, H) confirm that the overall textural structure is maintained, although the mold displays slightly broader curvature distributions, reflecting marginally sharper asperities. These small deviations are consistent with the general trend observed for the statistical moments discussed above, and confirm that, for the analyzed samples, PVS molds tend to slightly overestimate roughness and curvature variance, with a minor amplification of asperity sharpness, while preserving the general topographic characteristics of the surfaces.

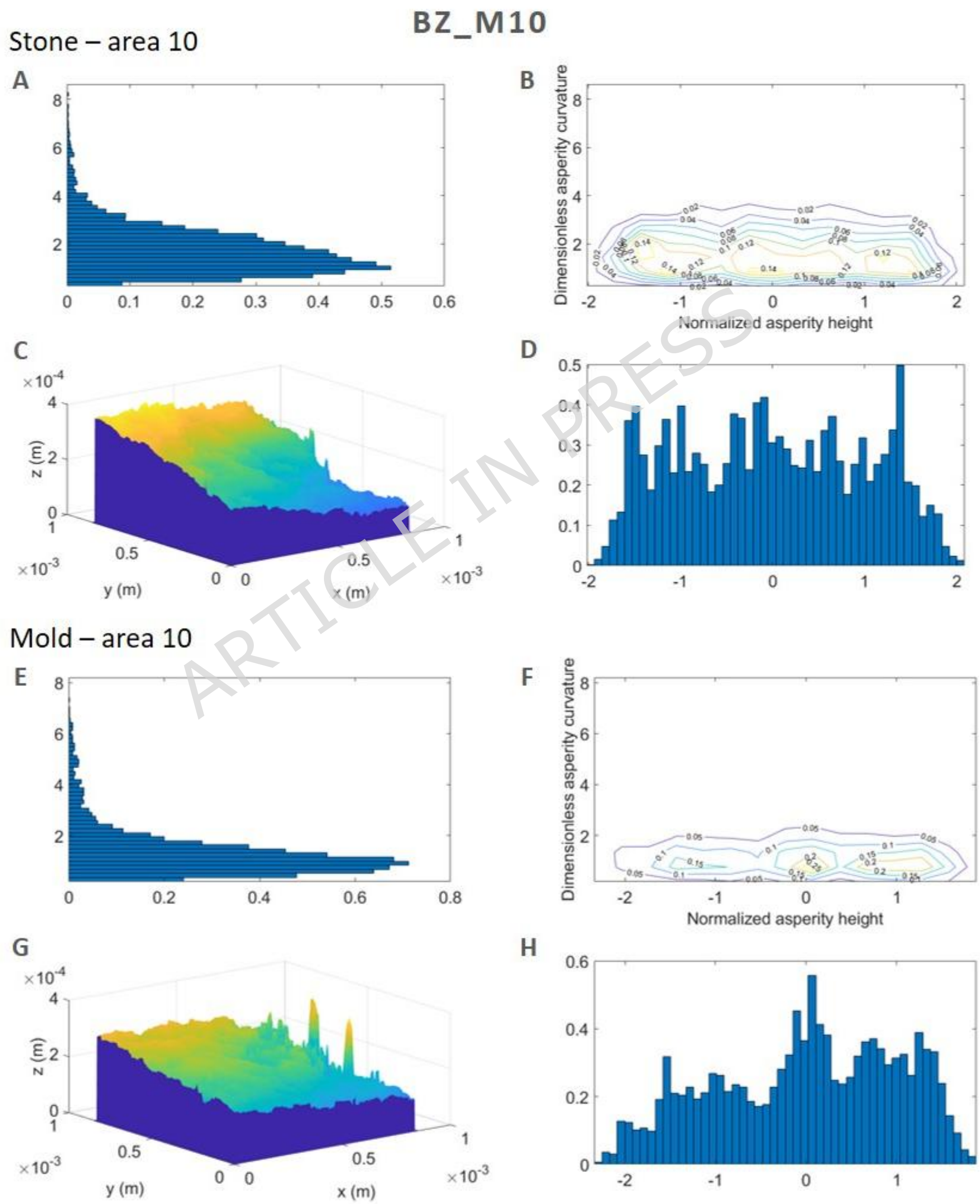

Figure 5. Comparative surface analyses for sample BZ_M10, showing area 10 on the original stone (A-D) and approximately the same area on the PVS mold (E-H). The analysis includes the asperity height distributions (A, E), curvature–height joint probability distribution contour plots (B, F), 3D microtopographic maps (C, G), and asperity curvature distributions (D, H).

Moreover, for DZU5_S and Vi1—selected as the most and least porous rocks respectively, and the most complex to analyze—a second mold (named Mold 2) was created and scanned for both samples to assess the accuracy of successive molds. In the case of DZU5_S, the Mold 2 exhibited numerous bubbles that made data acquisition not possible. This is probably attributable to the grease-like patina that PVS leaves on the stone surface after curing and peeling, which cannot be removed by simple washing or brushing. This residue, which seems more pronounced on porous stones, may compromise the complete adherence of a subsequent mold to the lithic surface.

In contrast, the same procedure was successfully carried out on the less porous Vi1, despite the visible presence of a few bubbles, and the results are shown in Figure 6. Overall, Mold 2 reproduces the main microtopographic characteristics of the original stone surface with reasonable fidelity, however, compared with Mold 1, it exhibits distinct performance patterns (Figure 6, first column). Regarding m_0, Mold 1 closely matches the original surface, with only slight overestimation of roughness in a few areas. Mold 2 has a similar trend but shows a slightly stronger tendency toward roughness amplification. The slope variance displays greater dispersion, with Mold 1 showing both under- and overestimations but average values close to the 1:1 line. In contrast, Mold 2 systematically underestimates slope steepness, resulting in a smoother replicated surface and mean values farther from the line of equality. The computed m_4 reveal that Mold 2 reproduces asperity curvatures and therefore their shape more accurately, while Mold 1 tends to overestimate the asperity sharpness. Comparisons between Mold 1 and Mold 2 (Figure 6, second column) demonstrate a high degree of internal consistency, indicating good reproducibility of the molding procedure despite minor deviations in microtopographic detail. These results suggest that for samples Vi1, Mold 1 provides better accuracy for overall roughness and slope analyses (m_0, m_2), whereas Mold 2 performs more reliably for peak curvatures (m_4).

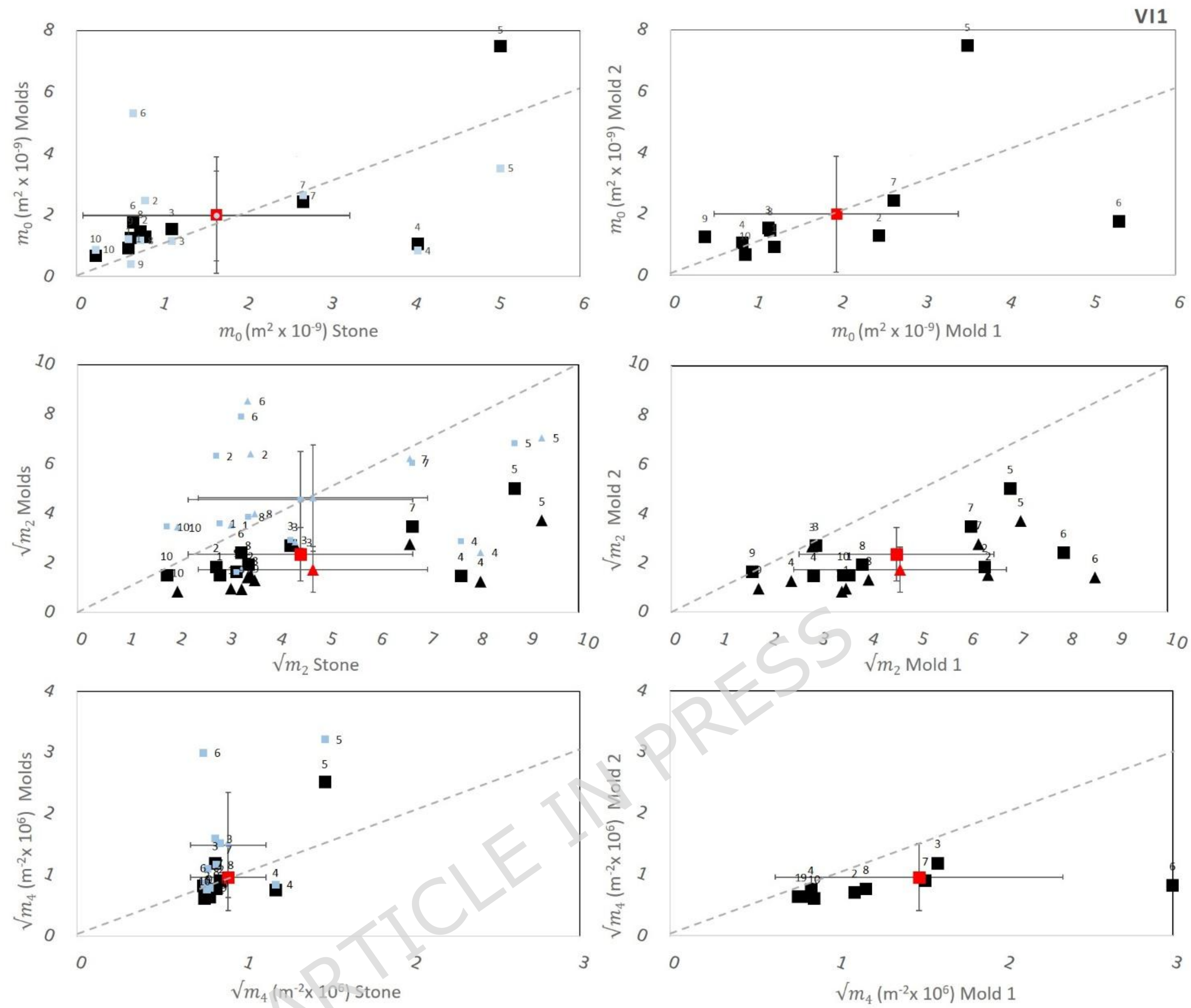

Figure 6. Scatter plots of the m₀, m₂, and m₄ parameters for sample Vi1. The first column compares the original lithic surface (x-axis) with approximately corresponding regions on Mold 2 (black markers, red mean values) on the y-axis, while Mold 1 (blue, smaller markers) is included for reference. The second column shows the comparison between Mold 1 (x-axis) and Mold 2 (y-axis). Error bars represent one standard deviation (±σ) calculated from ten microtopographic measurements. The dashed grey line indicates the 1:1 relationship between the compared datasets.

Furthermore, a second area on DZU5_S was scanned and molded twice using PVS that was previously stored in the refrigerator, to assess whether lower compound temperature affects replication accuracy by slowing the curing process. DZU5_S was selected as representing the more complex texture to be reproduced, both in terms of statistical parameters and air bubbles formation. The resulting negative imprints (two successive molds, named Molds 3 and 4) were then scanned (Figure 7).

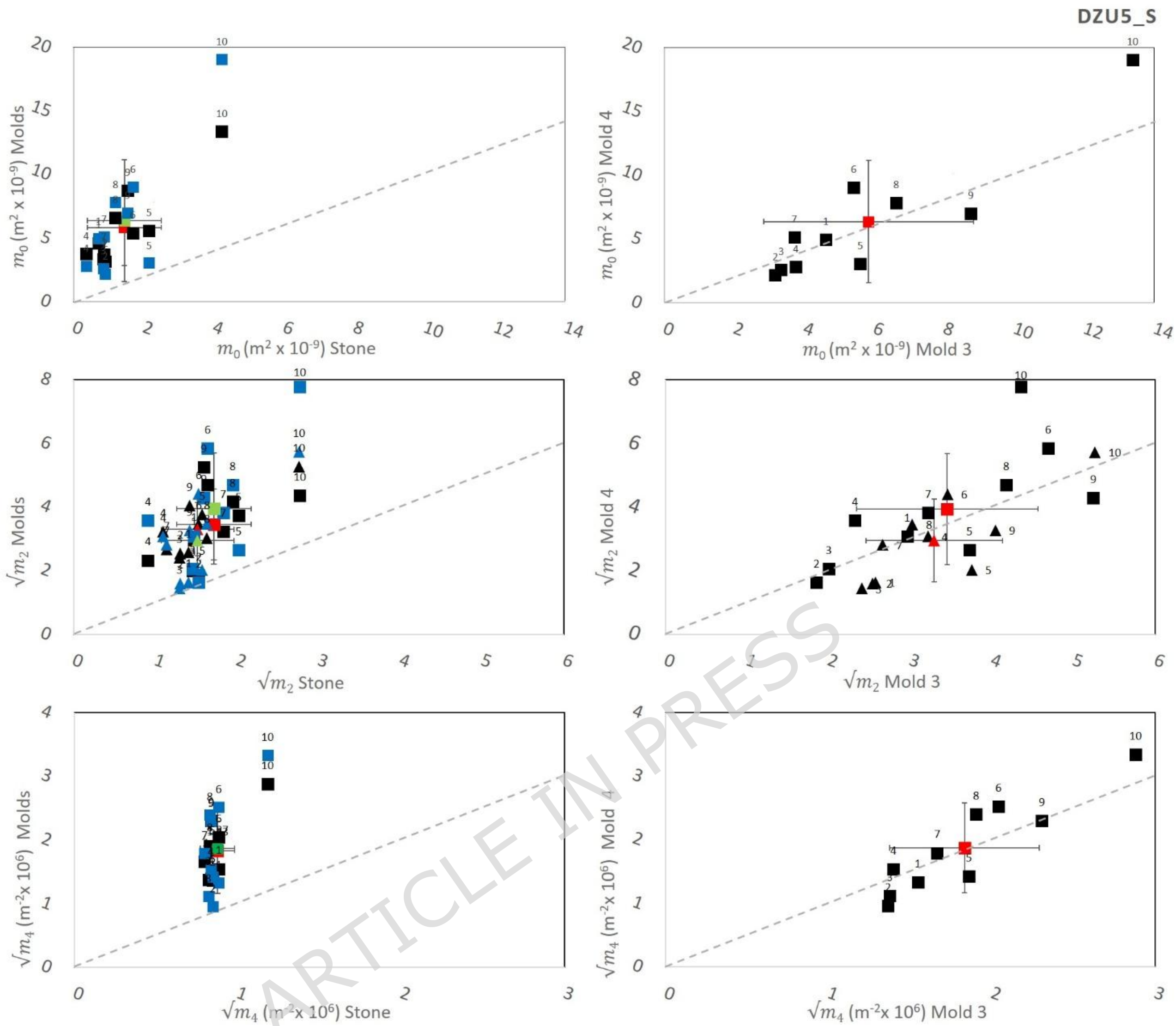

Figure 7. Scatter plots of the m_0, m_2, and m_4 parameters for sample DZU5_S. The first column compares the original lithic surface (x-axis) with approximately corresponding regions on Mold 3 (black markers, red mean) and Mold 4 (blue markers, green mean) on the y-axis. The second column presents comparisons between Mold 3 (x-axis) and Mold 4 (y-axis). Error bars represent one standard deviation (±σ) calculated from ten microtopographic measurements. The dashed grey line indicates the 1:1 relationship between compared datasets.

Both Mold 3 and Mold 4 reproduce the main microtopographic features of the original stone surface with overall good fidelity (Figure 7, first column). Mold 4 (the second impression), compared to Mold 3 (the first impression), shows a higher occurrence of air bubbles and noise spikes, likely increasing data variability—a pattern already observed for Mold 2 compared to Mold 1. Regarding m_0, both Mold 3 and 4 maintain a consistent correlation with the original surface but tend to slightly overestimate roughness amplitude, particularly in the case of Mold 4, as several values lie above the 1:1 line. Mold 3 shows tighter clustering around the equality line and a smaller average deviation, indicating more stable and precise replication of surface roughness. For m_2, both molds display a tendency to overestimate slope variance. Mold 3 exhibits a narrower spread and smaller standard deviations, reflecting higher precision and more consistent replication of slope steepness. Mold 4, by contrast, shows broader dispersion but includes several values lying closer to the line of equality, suggesting slightly higher accuracy but reduced precision. For m_4, both molds reproduce the asperity curvatures with reasonable accuracy; nevertheless, the majority of values lie above the 1:1 line, revealing a systematic bias toward sharpened peaks in the replicas. Mold 3 again displays tighter grouping, implying greater measurement precision, while Mold 4 shows a broader spread but includes more areas lying directly on the ideal 1:1 line, reflecting marginally higher accuracy in reproducing average curvature.

The comparison between Mold 3 and Mold 4 (Figure 7, second column) demonstrates a high level of internal consistency across all parameters, with values closely aligned along the line of equality. This confirms that the molding procedure is highly reproducible, despite minor differences in precision and accuracy between molds.

Overall, both molds yield reliable surface replicas, but Mold 3 performs slightly better overall, providing higher precision and more consistent replication across microtopographic metrics, whereas Mold 4 achieves comparable accuracy but exhibits an increased scatter likely linked to noise and microdefects introduced during molding.

Finally, to verify whether the mold kept at room temperature performed better than the one stored in the refrigerator, the deviation from the original stone surface was calculated for each of the three statistical moments for both Mold 1 and Mold 3 of DZU5_S, and their averages were compared. The results show that, although m_0 appears to be reproduced slightly better under cold conditions, the other parameters are more accurately reproduced by Mold 1. Furthermore, the standard deviation of the deviations confirmed higher reproducibility for the room-temperature mold. Consequently, the combined performance score indicates that Mold 1 performs slightly better overall for DZU5_S.

CONCLUSION

PVS is widely used in archaeology for its capability of reproducing fine surface details of artifacts, facilitating both transportation and analysis with fixed-design instruments. However, its effectiveness in replicating the complex surfaces of GSTs has remained largely unexplored, mainly due to the challenges posed by uneven surfaces and heterogeneous textures. To address this gap, we evaluated the intrinsic accuracy and precision of PVS molds and their suitability for quantitative analysis performed with confocal profilometry. This evaluation was conducted on four specimens representing lithologies, porosities, and surface morphologies comparable to archaeological GSTs from Upper Paleolithic contexts. The study also identified optimal molding conditions to improve replica accuracy for these lithologies, providing a methodological reference for future analyses of archaeological tools. Our results demonstrate that PVS is well suited for reproducing the microtopography of the selected lithic surfaces, although minor approximations should be acknowledged. Replication accuracy appears to decrease for highly porous lithotypes (e.g., DZU5_S), where localized amplification of surface roughness was observed, as indicated by slightly elevated m_0 values. In reflective quartz-based lithology (e.g., Vi1), minor deviations are more likely attributable to optical interferences during profilometric scanning rather than to inaccuracies in the PVS mold itself. Despite these limitations, the overall surface morphology and topographic trends of the four tested lithologies were consistently reproduced. Minor but systematic deviations between molds and original surfaces were nevertheless observed, typically expressed as a slight increase in the measured statistical moment values. Comparisons between first and second molds (i.e., Mold 1 vs. Mold 2 and Mold

3 vs. Mold 4) reveal a high degree of internal consistency, confirming that PVS replicas provide precise and reproducible data. Therefore, for quantitative evaluations, it is advisable to compare data between molds rather than between a mold and the original stone surface, thereby minimizing interpretative bias and ensuring uniform measurement conditions.

Although first and second molds are largely comparable, in this study, the latter generally exhibited increased noise, more frequent air bubbles, and a slightly greater approximation in the reproduction of microtopographic features. This may be due to minor damage caused during the detachment of the first mold, such as the removal of small stone particles, or the presence of residual PVS material retained in the deeper features of the surface, which can hinder the replicative accuracy of subsequent molds. Therefore, it is suggested to prioritize the first molds for quantitative analysis. However, archaeological tools typically carry residues (e.g., sediment and material processed with the tool) that can be captured by the first mold. To address this, the surface may be carefully cleaned—and any residues (e.g., starch) collected—prior to molding, although this procedure may introduce alterations to surface conditions and residual materials (see the *Samples selection and preparation* paragraph in the *Materials and Methods* section). Despite this trade-off, cleaning may improve the fidelity of the stone's texture replication by reducing the risk of incorporating extraneous material that could affect scanning and quantitative evaluation. Alternatively, for robust interpretation, datasets from multiple subsequent molds should be cross-referenced to quantify systematic deviations.

Finally, the comparison between molds produced from PVS stored at room temperature and at 6 °C, indicates that, on the tested lithotype, room-temperature PVS performs slightly better overall. While both storage conditions yield comparable m_0 values—reflecting similar accuracy in reproducing surface roughness—the room-temperature molds show greater fidelity for m_2 and m_4, indicating a better replication of slope and curvature characteristics.

MATERIALS AND METHODS

Samples selection and preparation

To assess the performance of PVS molding for quantitative microtopographic measurements of GSTs, using confocal profilometry as the analytical technique, four distinct rock types from different archaeological sites were selected for their similarity to real archaeological artifacts. The samples replicated the morphometric characteristics of both flat passive tools and active tools with rounded or convex surfaces, allowing assessment of whether the geometry and surface waviness influence PVS replication accuracy. Samples characteristics are reported in Table 1, including specimen name and provenance, images and dimensions, and petrographic description based on thin-section observation under transmitted light microscopy.

To measure the same area on both the stone surface and the mold, the definition of a reference feature was required. The challenge of precise spatial alignment is well recognized in archaeological surface texture studies, and several approaches have been proposed, including the use of attached ceramic beads as reference markers [55], permanent ink markings [25], and reference scratches on the surface [56-57]. In this study, an L-shaped reference feature measuring 0.5 x 1 cm was engraved on the stone to guide profilometric data acquisition.

Meticulous mechanical water-based cleaning prior to PVS application was crucial. Chemical agents were avoided to preserve surface integrity and prevent potential damage. Although mechanical brushing can modify lithic surfaces, as highlighted by previous research [58], this risk was negligible in the present study because unused specimens, lacking use-wear features, were employed. Removing soil and loose surface debris prior to molding was essential to minimize the possibility of residue entrapment in the PVS. The stones were initially brushed under running water and then placed in an ultrasonic bath (Brenson 5210) for a total of 90 minutes. In detail, each stone was individually placed in a zip bag filled with ultrapure water and set in the tank for three 30-minute baths. After each session, the water in the bag was changed, and the stone was rinsed under ultrapure running water [24]. Afterward, the stones were dried in an oven at 40°C for 48 hours to ensure complete drying and the absence of humidity that could affect mold polymerization time and accuracy [24, 44]. Throughout the process, the stones were handled with nitrile powder-free gloves to prevent surface contamination. The absence of latex in gloves is important to avoid potential interactions with PVS, which could inhibit polymerization [31].

Molding strategy

The selected PVS molding compound was Provil® Novo Light (Kulzer), primarily designed for dental applications due to its ability to create precise imprints of cavities, crevices, scarring, and undercuts. Along with President Jet by Coltène Whaledent, Provil® Novo is one of the most commonly used compounds in archaeological applications [44]. Since the viscosity of the silicone compound influences mold resolution [10, 38, 59], the light body variant was selected for its lower viscosity, allowing for better percolation into surface valleys and porosities [60]. This should result in a more accurate replication of surface details.

According to the manufacturer's published data, Provil® Novo offers excellent long-term dimensional stability, with a deformation under pressure of 3.1%, elastic recovery after deformation of 99.7%, and minimal distortion (linear shrinkage = -0.2%) [61]. The two-component compound (base and catalyst) is supplied in a cartridge and extruded through a 1:1 ratio mixing system, allowing approximately 90 seconds of working time before the polymerization process begins. The components may be manually mixed and applied to the stone surface with a spatula, or alternatively dispensed using an automixing tip directly onto the area to be replicated.

In this study, the automixing tip application method was used to address the well-known issue of bubble formation during molding, which can significantly impact quantitative analysis. By minimizing air incorporation during mixing, this approach should enhance mold accuracy. The paste was applied directly onto the areas to be copied, with the mixing tip held just above the surface, allowing the compound to flow slowly [62] and was then spread evenly with a spatula (Figure 1; Supplementary Video). Once applied to the L-shaped reference area on the stone surface, the mold was left to set and was easily peeled off after 150 seconds. This process was carried out in a temperature-monitored room (18–22°C), as previous studies [44] have identified this as the optimal temperature range for achieving high-fidelity molds.

Existing literature [16, 22, 63, 64] suggests that molds can peel away residue from stone surfaces, cleaning them. Consequently, it has been proposed that the same area be molded twice, reserving the second mold for traceological analysis. To further assess the robustness of this methodological approach, a second mold was prepared for DZU5_S and Vi1, representing the most and least porous rocks and the most analytically challenging samples, respectively. The replication was performed within minutes of the first molding to minimize potential dust deposition or environmental contamination of the lithic surface. However, after mold removal, a grease-like stain was observed on the copied areas of the stone surface, which may affect the accuracy of a second replication; its nature and impact are not addressed in this article.

Since lower temperatures delay polymerization [28, 44], additional tests were conducted using PVS stored at approximately 6°C. The aim was to provide the compound with more time to percolate into surface valleys, crevices, and pores, thereby reducing the risk of voids and bubbles. One such test was performed on a second L-shaped reference area of sample DZU5_S to assess the impact of pre-cooled PVS on mold fidelity.

The location of each mold on the stone surface was documented with photographs. Each mold was assigned a progressive identification number and stored in individual zip bags to prevent external particle contamination that could interfere with measurement accuracy. The lithic specimens were similarly stored in individual zip bags.

Analytical technique and data collection

To characterize the surfaces of both the stones and molds, microtopographic maps were acquired using the Leica DCM 3D dual-core 3D measuring microscope at the MUSAM-Lab, IMT School for Advanced Studies Lucca (Lucca, Italy). This instrument was chosen for its ability to measure surfaces across a wide range of scales, from several millimeters to a few nanometers, as well as its capability to analyze textures varying from smooth to highly rough with high measurement speed.

The Leica DCM 3D system operates in both confocal and interferometry modes; however, due to the high surface unevenness, the confocal mode was selected. Surface scans were performed using a 10x objective lens, capturing areas of 0.85 × 0.85 mm with a resolution of 512 × 512 data points. This lens has a numerical aperture (NA) of 0.30, a field of view (FOV) of 1270 × 950 µm, an optical resolution of 0.47 µm in the x/y plane, and a vertical resolution of <30 nm [65]. The selected magnification represents a compromise between achieving sufficient resolution and capturing a representative area within a single scan. Although the samples in this study were unused, 10× magnification was chosen to maintain methodological consistency with experimental or archaeological GSTs, where higher magnifications could risk capturing only part of a wear feature. While larger areas could, in principle, be scanned using the stitching option, this approach presents technical limitations, particularly in ensuring complete focus across the z-axis.

A sample of 14 areas were acquired along the L-shape scratch on each stone before molds. After the mold removal the negative copy of the same L-shape region was scanned on the molds (named Mold 1). Areas characterized by air bubbles were avoided. Since the scanning procedure relied on manual stage control, slight positional discrepancies occurred between the stone and the mold, precluding perfect spatial alignment of the scanned areas. All molds were scanned within 48 hours of curing to minimize any potential influence from dimensional changes [37]. Although the manufacturer's specifications indicate long-lasting dimensional stability, and the authors' experience suggests that PVS molds remain stable over extended periods, an early scanning was performed as a precautionary measure.

Additional tests were conducted to assess the accuracy of a second mold of the same area. The samples DZU5_S and Vi1, selected as the most and least porous rocks respectively, were used for this test. The region defined by the L-shaped feature was molded again (Mold 2) and scanned for both samples.

Furthermore, to evaluate whether the temperature of the PVS impacts its replication accuracy, a second L-shaped reference was drilled on DZU5_S and scanned. This area was then molded using PVS previously stored in a refrigerator, and the resulting negative imprint (named Mold 3) was scanned. The same areas were molded a second time (named Mold 4) to again investigate whether temperature variations may have an influence on the replication accuracy of successive molds.

It should be noted that for all tests, achieving a perfect correspondence between the areas on the molds and the stones was not possible, as the scanned spots have to be manually selected by the operator. However, the Leica DCM 3D allows for the acquisition of micrographs prior to scanning, supporting area selection and enabling alignment along the reference L-shaped feature.

Data processing and statistical analysis

Out of the 14 acquired areas per sample, at least 10 scans were free from mold bubbles and showed good correspondence between the scanned regions of the mold and the stone, as assessed using confocal micrographs. To ensure consistency across samples, 10 areas were therefore processed for each sample. The selected files were pre-processed in the open-source software Gwyddion (version 2.64) [66]. For the data obtained from the molds, a preliminary step involved flipping along the x-axis and inverting data value on the z-axis. This was necessary because the molds represent negative copies of the surfaces, requiring inversion to accurately simulate the actual tool surface and ensure comparability of the data. All the data were then exported in *.dat* format for analysis with a custom MATLAB-based procedure developed for roughness and contact mechanics studies, based on the theory described in [53]. Before analysis, all surfaces were detrended by removing the surface form using a first-order polynomial fit, which eliminates sample tilt. Subsequently, a smoothing filter with a radius of 1 was applied to reduce measurement noise. Acquisition artifacts were subsequently reduced using a smoothing filter implemented in the analysis algorithm (see `smoothing_function(x,y,z,radius,pt,tolp)` in the MATLAB scripts. The filter operates with a moving square window centered in a given point of the datagrid of indices i and j (i,j=1,...,512), with a lateral size equal to 2r, where r is the maximum number of adjacent grid points involved in the smoothing operation. Good results have been obtained with r=5. The filter operates by computing the average elevation $\bar{z}$ and the root mean square deviation σ over the heights contained within the filter window (i.e., r^2 heights). The elevation z_{ij} is then replaced by $\bar{z}$ if, and only if, it is higher than $\bar{z}+f\sigma$. The coefficient f (typically larger than 0.1 and lower than 3), which defines whether z_{ij} is considered an outlier requiring smoothing, is not defined a priori but it is computed by a bi-section algorithm. This procedure ensures that the maximum percentage of heights to be smoothed for a given surface is specified by the user. In the present study, this maximum threshold was set to 10% of the total heights. The coefficient f was automatically computed so that the same proportion of smoothed points was applied consistently across all surfaces. This filter is applied to all interior points of the surface except those belonging to the four outer rings near the boundaries, where the filter window would require modification (i.e., r<5). This modification of the filter was tested to address these boundary cases; however, the improvement was marginal in terms of the computed moments of the PSD function and the

joint distribution functions (e.g., Fig. 5 G). This is because outliers located near the surface boundaries represent only a very small fraction of the total elevations used to compute the surface statistics.
Three main spectral moments were finally calculated and plotted to statistically describe the roughness of the GSTs and enable comparison between the lithic surfaces and their molds (Table 2).

Table 2. Statistical parameters calculated and reported in the graphs, with their descriptions, formulas, and measurement units.

Parameter	**Description**	**Formula**	**Units of measure**
L	Lateral size of the acquired surface sample	-	m
δ	Sampling interval	*L/N*	m
N	Number of sampled heights per side	-	-
m_0	Variance of surface heights	$m_0 = \sum_{i=1}^{N} \frac{(z_i - \mu_z)^2}{N}$	m^2
m_2	Variance of the profile slopes (computed along profiles extracted along direction *x* or *y*)	$m_2 = \sum_{i=1}^{N_s} \frac{(s_i - \mu_s)^2}{N_s}$ $s_i = \frac{(z_{i+1} - z_{i-1})}{2\delta}$	-
m_4	Variance of the curvatures of the profile peaks (local maxima) computed along profiles extracted along direction *x*	$m_4 = \sum_{i=1}^{N_c} \frac{(c_i - \mu_c)^2}{N_c}$ $c_i = -\frac{(z_{i+1} - 2z_i + z_{i-1})}{\delta^2}$	m^{-2}

The zeroth spectral moment (m_0) represents the variance of surface heights, quantifying the overall vertical variance of asperities (peaks and valleys), with $z = 0$ corresponding to the deepest valley of the surface. The second spectral moment (m_2) reflects the variance of surface slopes, providing a measure of how steep or abrupt the asperities are. A higher m_2 values indicate greater slope variability and a more jagged surface texture, while lower values correspond to smoother microtopography. The fourth spectral moment (m_4) corresponds to the variance of asperity curvatures. High m_4 values indicate sharp, pointed asperities, whereas low values describe more rounded summit geometries [52]. In this study, m_4 is reported only along the x-direction, as profiles extracted along the y-direction were highly comparable. It is worth recalling that 512 profiles were acquired along both the x- and y-axes, and each profile contained 512 height data points.
In addition to the numerical descriptors, the MATLAB code also generates graphical outputs, including histograms, contour plots, and false-color microtopographical surface maps, which complement the statistical characterization of both GSTs and molds [53-54]. Two types of histograms are produced: one showing the statistical distribution of asperity curvatures, and the other displaying normalized asperity heights. These highlight differences in the frequency of sharp versus rounded features and in the relative abundance of high or low asperities. Contour plots depict the joint probability distribution of normalized

asperity height and dimensionless curvature, linking peak sharpness with relative elevation. Three-dimensional surface maps visually illustrate the topographic variation across the measured area, allowing an intuitive appraisal of height differences between stone and mold replicas. Together, these visualizations enrich the interpretation of the spectral moments and support a more direct comparison between original lithic surfaces and their molded copies.

ACKNOWLEDGEMENT

The authors gratefully acknowledge Alberto Conventi (Iuav University of Venice) for preparing the thin section for petrographic analysis.

Author contributions

Conceptualization, G.S.; Methodology, G.S., M.P.; Data curation, G.S., M.P.; Formal analysis, G.S., M.P.; Investigation, G.S., M.P., F.A.; Resources, G.S., M.P., L.L., A.M., E.B.; Funding Acquisition, M.P., E.B.; Validation, M.P., E.B.; Visualization, G.S., M.P.; Writing original draft, G.S., M.P., E.B.; Writing review and editing, G.S., M.P., L.L., F.A., A.M., E.B., all authors have read and agreed to the published version of the manuscript.

Funding

This study was performed with the support of *SMarT4BioArCH* project: *Ministero dell'Università e della Ricerca* of Italy, Project PRIN2022 2022XX8BRT PNRR, CUP Master B53DZ3014020006. Next Generation EU, is gratefully acknowledged for financial support.

Competing interests

The author(s) declare no competing interests.

Data availability statement

The MATLAB R2022 code used in this study, together with subsequent updates, is available on GitHub: https://github.com/marcopaggi/PVS_copy-capacity.git

The data underlying this study are openly available on Zenodo: https://doi.org/10.5281/zenodo.20732089

Supplementary Information

Supplementary Video S1. Mold preparation procedure.

REFERENCES

[1] Rose J.J. (1983). A replication technique for scanning electron microscopy: Applications for anthropologists. American Journal of Physical Anthropology, 62(3), 255–261. DOI: 10.1002/ajpa.1330620305.

[2] Bromage T.G. (1986). The Scanning Electron Microscopy/Replica Technique and Recent Applications to the Study of Fossil Bone. Scanning Microscopy, 1(2). Available at: https://digitalcommons.usu.edu/microscopy/vol1/iss2/17.

[3] Longo L. (1994) Le industrie litiche. L'analisi delle tracce d'uso. In: C. Peretto (Ed.), Le industrie litiche del giacimento paleolitico di Isernia la Pineta. La tipologia, le tracce di utilizzazione, la sperimentazione, Cosmo Iannone, Isernia, 355-404

[4] Ungar P.S., Teaford M.F. (1996). Preliminary examination of non-occlusal dental microwear in anthropoids: Implications for the study of fossil primates. Am. J. Phys. Anthropol., 100, 101-113. DOI: https://doi.org/10.1002/(SICI)1096-8644(199605)100:1<101::AID-AJPA10>3.0.CO;2-4

[5] Ungar P.S., Brown C.A., Bergstrom T.S., Walker A. (2003), Quantification of Dental Microwear by Tandem Scanning Confocal Microscopy and Scale-Sensitive Fractal Analyses. Scanning, 25, 185-193. DOI: https://doi.org/10.1002/sca.4950250405.

[6] Scott R., Ungar P., Bergstrom T. et al. (2005). Dental microwear texture analysis shows within-species diet variability in fossil hominins. Nature, 436, 693–695. DOI: https://doi.org/10.1038/nature03822

[7] Tumung L., Bazgir B., Ahmadi K., Shadmehr A. (2012). Understanding the Use-wears on Non-retouched Shells *Mytilus galloprovincialis*. and *Ruditapes decussatus* by Performing Wood Working Experiment: An Experimental Approach. IOP Conf. Ser.: Mater. Sci. Eng., 37, 012017. Doi:10.1088/1757-899X/37/1/012017

[8] Asryan L., Ollé A., Moloney N. (2014). Reality and confusion in the recognition of post-depositional alterations and use-wear: an experimental approach on basalt tools. Journal of Lithic Studies, 1(1), 9-32. DOI: https://doi.org/10.2218/jls.v1i1.815

[9] Ollé A., Vergèès J.M. (2014). The use of sequential experiments and SEM in documenting stone tool microwear. J. Archaeol. Sci., 48, pp. 60-72. DOI: https://doi.org/10.1016/j.jas.2013.10.028.

[10] Goodall R.H., Darras L.P., Purnell M.A. (2015). Accuracy and Precision of Silicon Based Impression Media for Quantitative Areal Texture Analysis. Sci. Rep., 5: 10800. DOI: https://doi.org/10.1038/srep10800.

[11] Pedergnana A., Ollé A. (2017). Monitoring and interpreting the use-wear formation processes on quartzite flakes through sequential experiments. Quat. Int, 427, pp. 25-65. DOI: http://dx.doi.org/10.1016/j.quaint.2016.01.052.

[12] Delgado-Raack S., de Tobaruela J.M., Bettinardi I., Soldevilla J.A., Risch R. (2022). Surface roughness as a quantitative approach to use-wear on macrolithic tools: A comparative analysis. J. Archaeol. Sci. Rep., 46, 102645. DOI: https://doi.org/10.1016/j.jasrep.2022.103645.

[13] Bofill M. (2012). Quantitative analysis of use-wear patterns: a functional approach to the study of grinding stones. In: Broadening Horizon. Conference of young researchers working in the Ancient Near East. Universitat Autònoma de Barcelona, Belleterra, 63-84.

[14] Adams J.L., Delgado-Raack S., Dubreuil L., Hamon C., Plisson H., Risch R. (2009). Functional analysis of macro-lithic artefacts: a focus on working surface. In: Non-flint raw material use in prehistory old prejudices and new direction, Proceedings of UISPP congress, Lisbon, Portugal, September 2006, Sternke F., Eigeland L., Costa L.J. (Eds.), BAR-IS, 43-66. ISBN: 978 1 4073 0419 9.

[15] Fullagar R., Wallis L. (2011). Use wear and phytoliths on bedrock grinding patches in North-Western Australia. In L. Russel (Ed.), Papers in Honor of Beth Gott.

[16] Dubreuil L., Savage D., Delgado-Raack S., Plisson H., Stephenson B., De La Torre I. (2015). Current analytical frameworks for studies of use–wear on ground stone tools. In: Use-wear and residue

analysis in archaeology; João Manuel Marreiros, Juan F. Gibaja Bao, Nuno Ferreira Bicho, Eds. Springer Cham, 105–158.

[17]Fullagar R., Stephenson B., Hayes E. (2017). Grinding grounds: Function and distribution of grinding stones from an open site in the Pilbara, western Australia. Quaternary International, 427, Part B, 175-183. DOI: https://doi.org/10.1016/j.quaint.2015.11.141.

[18]Hayes E.H., Pardo C., Fullagar R. (2018). Sandstone grinding/pounding tools: Use-trace reference libraries and Australian archaeological applications. J. Archaeol. Sci. Rep., 20, 97-114. DOI: https://doi.org/10.1016/j.jasrep.2018.04.021.

[19]Hayes E.H., Fullagar R., Field J.H., Coster A.C.F., Matheson C., Nango M., Djandjomerr D., Marwick B., Wallis L.A., Smith M.A., Clarkson C. (2022). 65,000-years of continuous grinding stone use at Madjedbebe, Northern Australia. Sci. Rep., 12, 11747.

[20]Cristiani E., Zupancich A. (2020). Sandstone Ground Stone Technology: a Multi-level Use Wear and Residue Approach to Investigate the Function of Pounding and Grinding Tools. J. Archaeol., 28, 704-725. DOI: 10.1028/s41598-020-72276-0.

[21]Chondrou D., Bofill M., Procopiou H., Vargiolu R., Zahouani H., Valamoti S.M. (2021). How do you like your cereal? A qualitative and quantitative use-wear analysis on archaeological grinding tools from prehistoric Greek sites. Wear, 476, 203636. DOI: https://doi.org/10.1016/j.wear.2021.203636.

[22]Longo L., Altieri S., Birarda G., Cagnato C., Cefarin N., Graziani V., Obada T., Pantyukhina I., Ricci P., Skakun N., Sorrentino G., Terekhina V., Tortora L., Vaccari L., Lubritto C. (2021). A Multi-Dimensional Approach to Investigate Use-Related Biogenic Residues on Palaeolithic Ground Stone Tools. Environ. Archaeol. DOI: https://doi.org/10.1080/14614103.2021.1975252.

[23]Longo L., Skakun N.N., Pantyukhina I.E., Terekhina V.V, Sorrentino G. (2021). Aurignacian grinding stone from Surein I (Crimea): "trace-ing" the roots of starch-based diet. J. Archaeol. Sci.Rep., 38, 102999. DOI: https://doi.org/10.1016/j.jasrep.2021.102999.

[24]Sorrentino G., Longo L., Obada T., Borghi A., Re A., Paggi M., Lo Giudice A. (2023). Tracing Old Gestures: A Multiscale Analysis of Ground Stone Tools Developed on Sequential Lab-Controlled Replicative Experiments. Heritage, 6, 4737–4767. DOI: doi.org/10.3390/heritage6060252.

[25]Sorrentino G., Longo L., Lo Giudice A., Re A., Paggi M. (2024). Replicative experimental use of Paleolithic Ground Stone Tools: Tracing and quantifying wear. Journal of Archaeological Science: Reports., 57, 104669. DOI: doi.org/10.1016/j.jasrep.2024.104669.

[26]Zupancich A., Cristiani E., Carra M., Antonović D., Borić D. (2025). Mesolithic plant processing unveiled: Multiscale use-wear analysis of the ground stone tools from Vlasac (Serbia). J. Archaeol. Sci.Rep., 61, 104907. DOI: https://doi.org/10.1016/j.jasrep.2024.104907.

[27]Wassell R.W., Ibbetson R.J. (1991). The accuracy of polyvinyl siloxane impressions made with standard and reinforced stock trays. The Journal of Prosthetic Dentistry, 65(6), 748-757. DOI: https://doi.org/10.1016/S0022-3913(05)80006-X.

[28]Chee W.W.L., Donovan T.E. (1992). Polyvinyl siloxane impression materials: A review of properties and techniques. The Journal of Prosthetic Dentistry, 68(5), 728-732. DOI: https://doi.org/10.1016/0022-3913(92)90192-D.

[29]Banks W.E., Kay M. (2003). High-Resolution Casts for Lithic Use-Wear Analysis. Lithic Technology, 28(1), 27–34. DOI: https://doi.org/10.1080/01977261.2003.11721000.

[30]Singer L., Habib S.I., Shalaby H.E., Saniour S.H., Bourauel C. (2022). Digital assessment of properties of the three different generations of dental elastomeric impression materials. BMC Oral Health, 22(1), 379. DOI: 10.1186/s12903-022-02419-4.

[31]Jadeja S.P., Austin R.S., Bartlett D.W. (2023). Use of polyvinyl siloxane impressions to monitor sub-5-µm erosive tooth wear on unpolished enamel. The Journal of Prosthetic Dentistry, 133(2), 577-583. DOI: https://doi.org/10.1016/j.prosdent.2023.04.020.

[32]Donovan T.E., Sulaiman T.A., Oliveira G.M.S., Bayne S.C., Thompson J.Y. (2019). Dental Biomaterials. In: Ritter A.V., Boushell L.W., Walter R. (Eds), Sturdevant's Art and Science of Operative Dentistry, Elsevier, 453-510. DOI: https://doi.org/10.1016/B978-0-323-47833-5.00013-7.

[33]Singer L., Bourauel C., Habib S.I., Shalaby H.E.A., Saniour S.H. (2022). Tear strength and elastic recovery of new generation hybrid elastomeric impression material: A comparative study. BMC Res Notes 15, 224. DOI: https://doi.org/10.1186/s13104-022-06110-3.

[34]Galbany J., Estebaranz F., Martínez L.M., Romero A., De Juan J., Turbón D., Pérez-Pérez A. (2006). Comparative analysis of dental enamel polyvinylsiloxane impression and polyurethane casting methods for SEM research. Microsc. Res. Tech. 69, 246–252. DOI: 10.1002/jemt.20296.

[35]Rodriguez J.M., Curtis R.V., Bartlett D.W. (2009). Surface roughness of impression materials and dental stones scanned by non-contacting laser profilometry. Dental Material, 25, 500-505. DOI: 10.1016/j.dental.2008.10.003.

[36]Bello S.M., Verveniotou E., Cornish L., Parfitt S.A. (2011). 3-Dimensional microscope analysis of bone and tooth surface modifications: comparisons of fossil specimens and replicas. Scanning 33, 316–324. DOI: 10.1002/sca.20248.

[37]Rodriguez J.M., Bartlett D.W. (2011). The dimensional stability of impression materials and its effect on in vitro tooth wear studies. Dent Mater. Mar, 27(3), 253-258. DOI: 10.1016/j.dental.2010.10.010.

[38]Macdonald D.A., Harman R., Evans A.A. (2018). Replicating surface texture: Preliminary testing of molding compound accuracy for surface measurements. J. Archaeol. Sci. Rep., 18, 839–846. DOI: https://doi.org/10.1016/j.jasrep.2018.02.033.

[39]Mihlbachler M.C., Foy M., Beatty B.L. (2019). Surface Replication, Fidelity and Data Loss in Traditional Dental Microwear and Dental Microwear Texture Analysis. Sci Rep 9, 1595. DOI: https://doi.org/10.1038/s41598-018-37682-5.

[40]Sawaura R., Kimura Y., Kubo M.O. (2022). Accuracy of dental microwear impressions by physical properties of silicone materials. Front. Ecol. Evol. 0:975283. DOI: 10.3389/fevo.2022.975283.

[41]Fullagar R., Grey C. (1983). Current research on the application of moulding techniques to use-wear analysis: notes. The Artefact: Journal of the Archaeological and Anthropological Society of Victoria, 8(1-2), 65–67.

[42]Rodriguez A., Iovita R. (2025). The good, the bad, and the bumpy: Evaluating the surface roughness accuracy of molding compounds for lithic use-wear analysis. SocArXiv. doi.org/10.31235/osf.io/r28yt_v1

[43]Pichon F., Ibàñez Estevez J. J., Anderson P., Abbés F. (2026). Assessing the reliability of silicone replicas in the analysis of sickle gloss at the early Neolithic site of Cheikh Hassan (Northern Levant,

11th millennium BP). Journal of archaeological science, 185(106446), 106446. DOI: https://doi.org/10.1016/j.jas.2025.106446

[44]Camarós E., Sánchez-Hernández C., Rivals F. (2016). Make it Clear: Molds, Transparent Casts and Lightning Techniques for Stereomicroscopic Analysis of Taphonomic Modifications on Bone Surfaces. Journal of Anthropological Sciences, 94, 1-8. DOI: 10.4436/jass.94023.

[45]Bar-Yosef O., Belfer-Cohen A., Mesheviliani T., et al. (2011). Dzudzuana: an Upper Palaeolithic cave site in the Caucasus foothills (Georgia). Antiquity, 85(328), 331-349. DOI: 10.1017/S0003598X0006779X.

[46]Baills H., Magniez P., Coppola D. (2021). Les occupations gravettiennes de la Grotte Santa Maria di Agnano (Pouilles, Italie) – Zone SMA-Esterno: typo-technologie lithique et archéozoologie, L'Anthropologie, 125(2), 102853. DOI: https://doi.org/10.1016/j.anthro.2021.102853.

[47]Allsworth-Jones P., Borziac I.A., Chetraru N.A., French C.A.I., Medyanik S.I. (2018). Brînzeni: A Multidisciplinary Study of an Upper Palaeolithic site in Moldova. Proceedings of the Prehistoric Society, 84, 41–76. DOI: https://doi.org/10.1017/ppr.2018.3.

[48]Karavanić I., Banda M., Radović S., Miko S., Vukosavljević N., Razum I., Smith F.H. (2021). A palaeoecological view of the last Neanderthals at the crossroads of south-central Europe and the central Mediterranean: long-term stability or pronounced environmental change with human responses. J. Quaternary Sci., 1–10. DOI: 10.1002/jqs.3279.

[49]Longo L, Veronese M, Cagnato C, Sorrentino G, Tetruashvili A, Belfer-Cohen A, et al. (2025) Direct evidence for processing Isatis tinctoria L., a non-nutritional plant, 32–34,000 years ago. PLoS One 20(5): e0321262. DOI: https://doi.org/10.1371/journal.pone.0321262.

[50]Leach R. (2011). Optical Measurement of Surface Topography. Springer Berlin Heidelberg. https://doi.org/10.1007/978-3-642-12012-1

[51]Zavarise G., Borri-Brunetto M., Paggi M. (2004) On the reliability of microscopical contact models, Wear 257 (3-4), 229-245. Doi: https://doi.org/10.1016/j.wear.2003.12.010

[52]Ma X., de Rooij M., Schipper D. (2010). A load dependent friction model for fully plastic contact conditions. Wear, 269, 790-796. DOI: https://doi.org/10.1016/j.wear.2010.08.005.

[53]Borri C., Paggi M. (2015). Topological characterization of antireflective and hydrophobic rough surfaces: are random process theory and fractal modeling applicable? J. Phys. D: Appl. Phys., 48, 045301. DOI: 10.1088/0022-3727/48/4/045301.

[54]Greenwood J.A. (2006). A simplified elliptic model of rough surface contact, Wear, 261(2), 191-200. DOI: https://doi.org/10.1016/j.wear.2005.09.031.

[55]Calandra I., Schunk L., Rodriguez A., Gneisinger W., Pedergnana A., Paixão E., Pereira T., Iovita R., Marreiros J. (2019). Back to the edge: relative coordinate system for use-wear analysis. Archaeological and Anthropological Sciences, 11, 5937–5948. https://doi.org/10.1007/s12520-019-00801-y

[56]Stemp W.J., Stemp M. (2003). Documenting stages of polish development on experimental stone tools: surface characterization by fractal geometry using UBM laser profilometry. J. Archaeol. Sci., 30, 287-296. DOI: https://doi.org/10.1006/jasc.2002.0837.

[57]Martisius N.L., Sidéra I., Grote M.N., Steele T.E., McPherron S.P., Schulz-Kornas E. (2018). Time wears on: assessing how bone wears using 3D surface texture analysis. PLoS One, 13, e0206078. DOI: https://doi.org/10.1371/journal.pone.0206078.

[58]Pedergnana A., Calandra I., Bob K., et al. (2020). Evaluating the Microscopic Effect of Brushing Stone Tools as a Cleaning Procedure. Quaternary International, vol. 569-570: 263-76. DOI: doi.org/10.1016/j.quaint.2020.06.031

[59]del Campo A., Álvarez I., Filipe S., Wilhelm M. (2007). 3D Microstructured Surfaces Obtained by Soft-Lithography Using Fast-Crosslinking Elastomeric Precursors and 2D Masters. Adv. Funct. Mater., 17, 3590-3597. DOI: https://doi.org/10.1002/adfm.200700132.

[60]Valtierra N., Courtenay L. A., Yravedra J., López-Polín L. (2023). Cumulative effect of high-resolution silicone moulds on the morphology of cut marks. Archaeometry, 66(3), 665–682. DOI: https://doi.org/10.1111/arcm.12938.

[61]Kulzer Mitsui chemicals group (2021). Provil novo: Informazione prodotto (accessed on 16th Februray 2023). Available online at: kulzer-dental.it/IT/downloads/further_products_2/provil_1/Provilnovo_ProdInfo_Logo_Kulzer.pdf.

[62]Sturdevant J.R. (2019). 18 - Class II Cast-Metal Restorations. In: Ritter A.V., Boushell L.W., Walter R. (Eds), Sturdevant's Art and Science of Operative Dentistry, Elsevier, e94-e154. ISBN 9780323478335. DOI: https://doi.org/10.1016/B978-0-323-47833-5.00018-6.

[63]Solounias N., Semprebon G. (2002). Advances in the reconstruction of ungulate ecomorphology with application to early fossil equids. American Museum Novitates, 3366, 1–49. https://doi.org/10.1206/0003-0082(2002)366<0001:AITROU>2.0.CO;2.

[64]Evans A.A., Macdonald D.A., Giusca C.L., Leach R.K. (2014). New method development in prehistoric stone tool research: evaluating use duration and data analysis protocols. Micron, 65. pp. 69-75. DOI: 10.1016/j.micron.2014.04.006.

[65]Leica microsystem (2023). Leica DCM 3D. Available from: www.leica-microsystems.com.

[66]Nečas D., Klapetek P. (2012). Gwyddion: an open-source software for SPM data analysis. Cent. Eur. J. Phys., 10, 181–188. DOI: https://doi.org/10.2478/s11534-011-0096-2.